



Article citation info:

Witanowski Ł, Breńkacz Ł, Szewczuk-Krypa N, Dorosińska-Komor M, Puchalski B. Comparable analysis of PID controller settings in order to ensure reliable operation of active foil bearings. *Eksploracja i Niezawodność – Maintenance and Reliability* 2022; 24 (2): 377–385, <http://doi.org/10.17531/ein.2022.2.19>.

Comparable analysis of PID controller settings in order to ensure reliable operation of active foil bearings

Indexed by:



Łukasz Witanowski^a, Łukasz Breńkacz^{a,*}, Natalia Szewczuk-Krypa^b, Marta Dorosińska-Komor^b, Bartosz Puchalski^{c,d}

^aPolish Academy of Sciences, Institute of Fluid Flow Machinery, ul. Fiszerza 14, 80-283 Gdansk, Poland

^bGdansk University of Technology, Faculty of Mechanical Engineering and Ship Technology, Institute of Naval Architecture and Ocean Engineering, ul. Gabriela Narutowicza 11/12, 80-233 Gdansk, Poland

^cGdańsk University of Technology, Digital Technologies Center, ul. Gabriela Narutowicza 11/12, 80-233 Gdańsk, Poland

^dGdańsk University of Technology, Department of Intelligent Control and Decision Support Systems, Faculty of Electrical and Control Engineering, ul. Gabriela Narutowicza 11/12, 80-233 Gdańsk, Poland

Highlights

- An optimization of controller parameter to prevent failures.
- Prediction the behaviour of an active foil bearing controlled by PID controller.
- The stochastic and hybrid algorithms were used for optimization.
- This work could help prevent failures of active foil bearing.

Abstract

In comparison to the traditional solutions, active bearings offer great operating flexibility, ensure better operating conditions over a wider range of rotational speeds and are safe to use. In order to ensure optimum bearing performance a bearing control system is used that adapts different geometries during device operation. The selection of optimal controller parameters requires the use of modern optimization methods that make it possible to quickly achieve the assumed parameters. This article presents the method that has been employed to select the parameters of a proportional integral derivative (PID) controller, in which both stochastic algorithms and hybrid methods have been compared.

The results show that all of the used algorithms were able to reach the global optimum but only the hybrid algorithm was repeatable in all runs within a low value of the standard deviation. The best solution will be proposed in the future to control an active foil bearing. Analysing of this paper would help to prevent failures of active foil bearing used in the designed rotating machine.

Keywords

This is an open access article under the CC BY license (<https://creativecommons.org/licenses/by/4.0/>)

gas foil bearing, operation stability, PID controller, optimization, rotor dynamics, comparable analysis.

1. Introduction

Compared to conventional bearings, active bearings allow to minimize vibrations (especially in resonant modes), better compensate for temperature changes and improve operating safety. Despite these advantages the failures of active bearings can also occur and may break the continuity of production, destroy whole machine and even cause a major injury. In order to solve many problems concerning the operation and properties of foil bearings, FEM simulations are carried out by Peng et al. [44], among other activities, by coupling various fields such as mechanical and thermal [57]. Another way to improve the performance, efficiency and reliability of equipment with bearings in their systems is the use of an appropriate procedure to improve the predictive maintenance protocol [12]. The approach allows to increase the number of monthly tests, improving predictability, reliability, maintenance and production at the same cost. Other methods are

also used to determine the remaining service life of systems equipped with bearings, where stochastic, hybrid algorithms or machine learning elements are used. In the article Major et al. [35], the remaining working time was estimated using particle swarm optimized vector machines, taking into account two pre-processing techniques allowing to improve the quality of the input data, which consequently contributed to the generation of more accurate predictions.

There are many types of bearing designs allowing to control them, a few of them are considering by Breńkacz et al. [9]. The best known are magnetic bearings [54]. A comprehensive research on various types of both liquid and gas lubricated sliding bearings is underway [7, 42, 43, 58]. The common feature of these bearings is the control system, which also is implemented in many ways. Such control is carried out, for example, via controllers using fuzzy logic or neural controllers. Still, however, the use of PID controllers remains the most popular solution. Therefore, the work focused on this solution. The

(*) Corresponding author.

E-mail addresses: Ł. Witanowski (ORCID: 0000-0002-2921-6070): lwitanowski@imp.gda.pl, Ł. Breńkacz (ORCID: 0000-0001-7480-9636): lbrenkacz@imp.gda.pl, N. Szewczuk-Krypa (ORCID: 0000-0001-5824-0398): natalia.szewczuk@pg.edu.pl, M. Dorosińska-Komor (ORCID: 0000-0002-5614-1203): mardrosi@pg.edu.pl, B. Puchalski (ORCID: 0000-0001-9834-6250): bartosz.puchalski@pg.edu.pl

control quality indexes, including settling time, overshoot and, in general, the way the bearing works, depends on the selection of the operating parameters of the PID controller. The references to the selection of PID and PD controller parameters for magnetic bearings can be found in the paper [47] by Psonis et al., . They analysed linear controllers and their stability issues of closed loop system, using the Routh-Hurwitz criterion. The classic ways of determining the controllers settings include the Ziegler-Nichols (ZN) method were applied by Ahmad et al. [2] and Kushwah et al. [36]. The aim of this research work is to process the optimization of controller parameters in an active radial bearing.

Generally bearing control is very complicated due to the need for rapid changes of the system properties. Some scientific papers describing ways of controlling magnetic [53], hydrodynamic [23] and aerodynamic bearings [41] are available, but there is no literature [10] that would describe and comprehensively compare different types of optimization algorithms applied to determine the parameters of the PID controller operating in the control system of the active foil bearing. The issue addressed in the article paper utilizes various types of optimization algorithms, including stochastic, deterministic and hybrid ones, and shows what parameters of the PID controller have been determined with their use. It turned out that the values of the controller parameters vary depending on which optimization algorithm is used. These differences influence the dynamic properties of the rotor-bearing system, that are also shown in this paper.

In this case, a PID controller was selected for controlling the radial bearing. The controller scheme is presented in Fig. 1. As it can use feedback, it ensures the rejection of disturbances, eliminates the deviation in the steady state by means of integral contributor, and using derivative component, it reduces the oscillations of the controlled value [33]. In addition, 90% of industrial control loops are currently based on the PID control algorithm, which results in further scientific research on their development [30]. When selecting controller parameters, it is important to obtain appropriate values for settling time, overshoot and steady-state error (Fig. 2). The settling time is the time interval measured from the moment the disturbance is applied to the system or of a step change in the setpoint until the control error is within $\pm 5\%$ of the setpoint. The value of settling time percentage may vary depending on the application. Another important parameter is overshoot k , i.e. the percentage ratio of the two subsequent controlled value or error extremes ($e_2; e_1$). The overshoot is usually determined by a step change of the setpoint based on the following relationship:

$$\kappa = \frac{e_2}{e_1} * 100\% \quad (1)$$

The last, but not least important parameter is the steady state error Δr , which is determined by the difference between the setpoint and the controlled value after the steady state was reached, i.e. after the stabilization of the control system. Typically, the control systems aim at a zero steady state error.

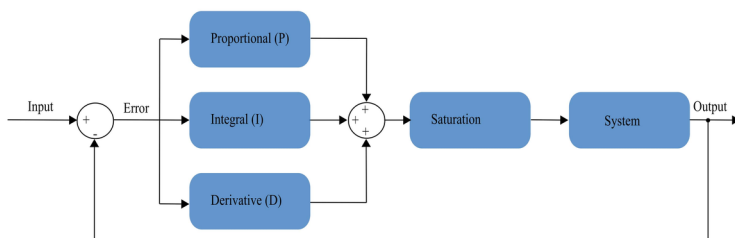


Fig. 1. Automatic control system making use of a PID controller

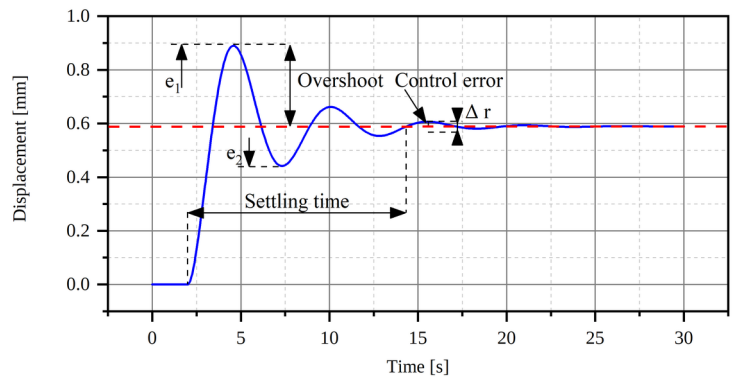


Fig. 2. Key control quality indexes when selecting PID controller parameters

There are two typical engineering methods for determining PID controller parameters [5]:

- 1) the method based on a delayed response of a first-order open-loop system to a unit step – the 1st ZN method;
- 2) the method of limit cycle tested in a closed-loop system – the 2nd ZN method.

The inventors of this method carried out many studies which resulted in the development of universal relationships for the choice of the P/PI/PID controller parameters. These relationships are presented in Table 1, where the setpoint depends on the controller $a = \frac{K}{L} * T$. The K , L and T parameters are obtained on the basis of the object's response to the step function [1, 3].

Table 1. Parameters based on the first Ziegler-Nichols method [3]

| Parameter | P | PI | PID |
|-----------|-------|---------|---------|
| K_p | $1/a$ | $0.9/a$ | $1.2/a$ |
| T_i | - | $3L$ | $2L$ |
| T_d | - | - | $L/2$ |

The limit cycle method is based on reaching the stability limit in a closed-loop control system. In order to use it in the closed-loop system, one should disable the integral and the derivative terms and set the gain so as to achieve constant amplitude oscillations with the period – P_u . The gain determined in this case is called the ultimate sensitivity K_u . In order to determine the parameters of PID controllers, the authors of this method developed the relationships presented in Table 2.

Table 2. Parameters based on the second Ziegler-Nichols method [46]

| Parameter | Unit | P | PI | PID |
|-----------|-------------------|-----------|------------|-----------|
| K_p | - | $0.5 K_u$ | $0.45 K_u$ | $0.6 K_u$ |
| K_i | min^{-1} | - | $1.2/P_u$ | $2/P_u$ |
| T_d | min | - | - | $P_u/8$ |

The Ziegler-Nichols methods are quite simple and intuitive, which can undoubtedly be considered an advantage. The main disadvantage is, however, a very low damping of the control system [6]. In subsequent years, papers presenting modifications of the Ziegler-Nichols method were published, including those made by Pessen [45], Chien together with Hrones and Reswick, [16]. Pessen modified the Ziegler-Nichols method by adopting the criterion of the aperiodic system response caused by the step function. After taking this criterion into account, the

values of K_p , K_i and T_d coefficients should be changed to the values consistent with ($S_u=k_{kr}$, $P_u=T_{kr}$), shown in Table 3.

Table 3. Controller parameters based on the Ziegler-Nichols method modified by Pessen (k_{kr} -ultimate sensitivity T_{kr} -critical vibration period)

| Parameter | P | Pi | PID |
|-----------|--------------|---------------|---------------|
| K_p | $0.2 k_{kr}$ | $0.15 k_{kr}$ | $0.2 k_{kr}$ |
| K_i | - | $0.4 T_{kr}$ | $0.33 T_{kr}$ |
| T_d | - | - | $0.5 T_{kr}$ |

Over the years, further studies on selection of the PID controller parameters were carried out. Astrom et al. [4] described the methods of PI controller parameters selection using non-convex methods. Optimization gain method [24] is obtained for two plots for which the intersection points are sought, these plots are obtained by using the frequency response of the process. This process is valid when one solution is assigned to the intersection of the plots Mendez et al. [37] presented several algorithms of automatic PID controller tuning using implicit and explicit identification algorithms. Modern tuning methods include those utilizing: genetic algorithms [50, 51, 55], fuzzy models [48, 49] and artificial neural networks [29].

There are papers on tuning the controllers utilized to control bearings by applying the methods mentioned above. In case of magnetic bearings, a self-tuning fuzzy PID controller is used, among others [14], where genetic algorithms are applied to determine its best parameters [13].

The Ziegler-Nichols method is usually one of the first methods used to determine controller parameters. In case of radial gas bearings analysed by the Authors of this paper, it was not possible to determine the parameters of the PID controller using this method. Therefore, different optimization algorithms were used to determine the PID controller parameters and the results are presented below in the paper. Stochastic and hybrid algorithms are often used in the issues of reliability and maintenance, but this was not the case before for active foil bearings [15, 52].

2. Radial bearing model

The analysed active foil bearing consists of a bush and a rotating shaft (Fig. 3). Between them there is a layer of lubricating film and a layer of the foil's structural support. Both layers can be represented in calculations by stiffness and damping coefficients. The gas film coefficients are marked with the G index, while the foil coefficients with the F index as marked in Fig. 3 a) and b) which introduces an equivalent model of the bearing by determining the replacement coefficients for the gas film and the foil layer supporting the bearing. The model with

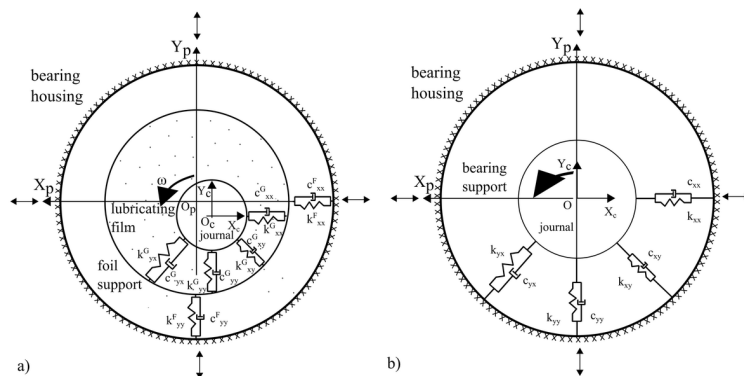


Fig. 3. Gas foil bearing: a) general scheme, b) equivalent model of the gas foil bearing used for control

equivalent stiffness and bearing damping coefficients was used for controller synthesis purposes.

In order to describe the connection between the rotor shaft and the bearing bush, the second order linear differential equation was applied (2). For this purpose, the equivalent stiffness, bearing damping coefficients and shaft weight were used. The excitation force was applied as a sine function with a frequency equal to the rotor speed and amplitude resulting from the residual unbalance:

$$M\ddot{p}(t) + (C + \Omega G)\dot{p}(t) + Kp(t) = f(t) \quad (2)$$

where:

- M – mass deposited on the bearing (reduced shaft weight transferred by the bearing),
- C – equivalent bearing damping,
- G – gyroscopic torque,
- K – equivalent stiffness of the bearing,
- Ω – rotational speed,
- $p(t)$ – displacement of the shaft,
- $f(t)$ – excitation force resulting from unbalance of the rotor.

2.1. Bearing model designing in Matlab SIMULINK environment

The model was developed in Matlab SIMULINK rapid prototyping computer environment [8]. The result is a displacement of the shaft in directions perpendicular to the bearing axis (p_{xx}, p_{yy}). Since the values of the main stiffness (k_{xx}, k_{yy}) and damping (c_{xx}, c_{yy}) coefficients are much higher than the values of the diagonal stiffness (k_{xy}, k_{yx}) and damping (c_{xy}, c_{yx}) coefficients, the latter were omitted. In the presented model changing the position of the actuator causes a change in diameter, which has a direct impact on the value of the damping coefficients and the stiffness of the gas film. The relationship between the bearing diameter and the stiffness and damping coefficients in both horizontal and vertical directions calculations were per-

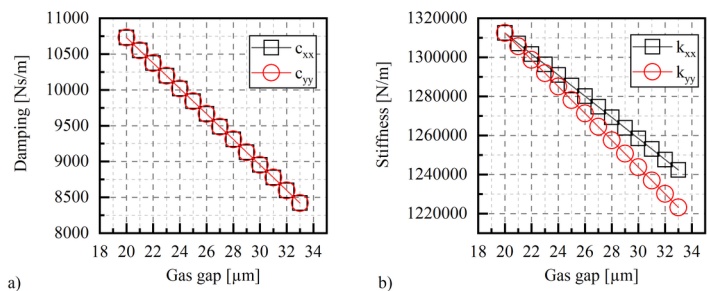


Fig. 4. a) Relationship between changes in damping (c_{xx}, c_{yy}) and b) stiffness (k_{xx}, k_{yy}) coefficients as a function of changes in lubrication gap diameter (r_{xx}, r_{yy})

formed in MESWIR [32]. Fig. 4. presents damping and stiffness coefficients as function of the lubrication gap for the rotational speed of 18,000 [rpm].

The sinusoidal dynamic external force acting on the shaft bearing system in the initial was assumed. The force depends on the speed and residual rotor unbalance, according to the formula:

$$F_{unbalance} = m_{un} \cdot r_{un} \cdot \Omega^2 \quad (3)$$

where:

- m_{un} — unbalance mass; r_{un} — unbalance radius; Ω — speed

The shaft displacement over time (sinusoidal signal) is related to the model's response to the input force and corresponds to

the vibration amplitude in the same direction. In the developed bearing model, the horizontal displacement (Fig. 5) p_{xx} and the vertical displacement p_{yy} are considered separate and independent of each other. Fig. 5 presents a block diagram of the bearing showing movements in one direction.

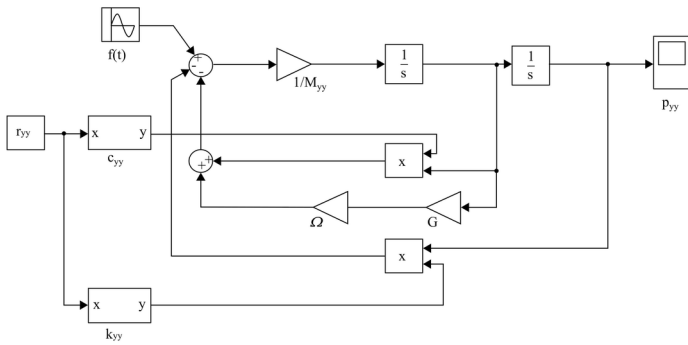


Fig. 5. Bearing model block diagram showing the displacement of a shaft in the direction p_{yy} due to an external sinusoidal force ($1/s$ – integrator; x – the product block, y – block output)

In the subsequent stages of model development, the external dynamic force acting on the bearing-shaft system was replaced by a static force. The amplitude value of this force was the same as the sinusoidal force amplitude value. This procedure was performed so that the influence of the dynamic force on the change of the rotor position is the same as the influence of the static force. A correction factor was introduced into the system. This made it possible to use a constant reference value instead of a sinusoidal value in the control system (because a constant value of the excitation force was used). This simplification can only be used at low speeds (in relation to the resonant speed). The bearing model shown in Fig. 5 was extended by the control system shown in Fig. 6. The tasks of the described system include the control and observation of the rotor vibration amplitude. The previously created model was equipped with a feedback loop controller. The controller acts on the actuator with a signal of appropriate voltage $U(t)$ by using the values obtained at a given moment in time from control error $e(t)$, vibration amplitude $p_r(t)$ and moment $p(t)$. The size of the lubrication gap depends on the displacement of the actuator $r(t)$ controlled by the voltage. The change in the vibration of the bearing results from the newly developed value of the coefficients of damping and stiffness of the lubricating film.

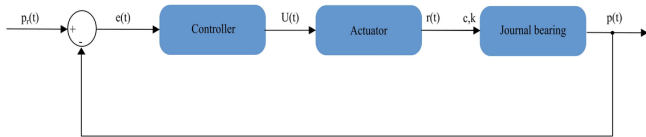


Fig. 6. Operation diagram of the control system

The system uses an actuator that can be used to force displacement in the range from 0 to 40 μm for current signal with voltage from 0 to 10 V. Piezoelectric material, a stepper motor, etc. can act as such an actuator. It is assumed that the dependence between the voltage change of the signal supplied to the actuator and the change of its position is linear. The displacement change in the horizontal and vertical direction is carried out independently by two autonomous, separately adjustable actuators. This means that the lubricating gap is always circular-cylindrical. The model shown in Fig. 7 uses a PID controller, whose parameters have been optimized, as presented in the next chapter. The system assumes a limitation of the controller's operation. The restrictions applied were to protect the control element from damage. In this case, it was assumed that the piezoelectric element responsible

for changing the lubricating gap should not receive a voltage signal of more than 10V from the control system. The signal limitation values are based on the safe working area of the actuator.

3. Methodology of selecting optimal PID controller parameters

3.1. Optimization algorithms

The Authors of paper compared seven optimization algorithms belonging to the groups of stochastic and hybrid algorithms, of which six methods belong to the first group and one to the second. Stochastic algorithms include methods in which the selected or all parameters of a given algorithm are random, or are dependent on random numbers. The most popular stochastic methods include genetic algorithms or algorithms based on swarm behaviour (e.g.: particle swarm algorithm, bee swarm algorithm) [22]. Hybrid algorithms, on the other hand, were created by combining various deterministic methods with various stochastic methods. It is also possible to combine only deterministic methods [34] or only stochastic methods. Hybrid algorithms can be divided due to their structure and principle of operation: cooperating and integrated [56].

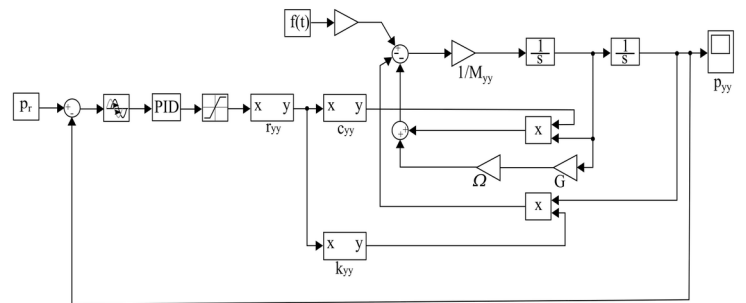


Fig. 7. Bearing block diagram showing the displacement of the shaft in the direction p_{yy} due to an external force, including the control system

Genetic algorithm (GA)

John Holland is considered to be the precursor of genetic algorithms [38]. In 1975, he was the first to present a simple example of a genetic algorithm, which was then developed by other scientists [21]. The greatest contribution to the further development of this algorithm was made by Goldberg [26]. These algorithms belong to the group of evolutionary algorithms [20] and are based on the knowledge resulting from the observation of nature and Darwin's idea of evolution, or more precisely, the mechanism of inheritance and natural selection of individuals, i.e. they follow the Darwin's idea.

Particle Swarm Optimization (PSO)

The algorithm considered by Kennedy and Eberhart [18] was created on the basis of observation and simulation of the behaviour of bird and fish clusters, carried out by Heppner and Tomer and Tu Ba [28]. This algorithm realizes directed motion of particles in space of a certain dimension, in search of an optimal solution for n decision variables (arguments of target function). The optimization process is carried out in an iterative way. Each of the particles determines its subsequent position on the basis of both its previous experience and that of the whole group [19]. In addition, the ability to memorize and thus return to previously known areas with convenient properties makes it possible to adapt particles to the environment. The process of particle swarm optimization consists in finding ever better particle positions in the search space and, as a result, finding the optimal position to which the whole group converges.

The Whale Optimization Algorithm (WOA)

The Whale Optimization Algorithm is a novel nature-inspired metaheuristic optimization method which mimics the social behaviour of humpback whales [39]. The method based on the bubble-net hunting strategy. The algorithm consists of encircling prey, spiral bubble-net feeding maneuver and search for prey.

Hybrid Grey Wolf and Cuckoo Search Optimization Algorithm (GWOCS)

The hybrid algorithm is a combination of Grey Wolf Algorithm and Cuckoo Search Algorithm [27]. The standard GWO algorithm tend to fall into local minima. In order to avoid this problem, the Cuckoo Search Algorithm was used.

Time Varying Acceleration Particle Swarm Optimization Algorithm (TACPSO)

The presented algorithm is a modification of the popular particle swarm optimization (PSO) algorithm [40]. The applied modification proposed a strategy for the adjustment of cognitive and social coefficients, which was defined as follows:

$$C_1 = 0.5 + 2e^{\left(-\left(4 \cdot \frac{1}{Max_{it}}\right)^2\right)} \quad (4)$$

$$C_2 = 2.2 - 2e^{\left(-\left(4 \cdot \frac{1}{Max_{it}}\right)^2\right)} \quad (5)$$

where:

Max_{it} – max number of iteration; C_1 – cognitive coefficient; C_2 – social coefficients.

The applied modification reduced the cognitive coefficient and increased the social coefficient with the progress of iteration (Fig. 8). Particles can move through the entire area of research assuming a large cognitive component and a small social component. On the other hand, the optimization process can also be lengthened with a social component that is too large and a cognitive component too small.

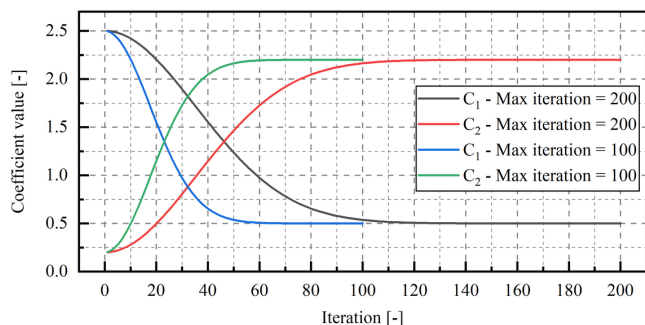


Fig. 8. Cognitive and social coefficients in a function of iteration number

Chimp algorithm (ChOA)

The Chimp algorithm is a novel metaheuristics intelligence algorithm based on the individual and sexual motivation of chimps, which is quite different from the other social predators during the hunt [31]. The algorithm was presented by Khishe and Mosavi in 2020 [31]. This form of society (a fission-fusion) is characterized by dynamic property composition and size of the group [17]. This method based on independently searching by each created group of chimps which are different in intelligence and ability.

Turbulent Flow of Water-based optimization (TFWO)

The TFWO algorithm was proposed in 2020 for the first time by Ghasemmi et al. [25]. This optimization method based on whirlpool phenomenon created in a turbulent flow of water[25]. In the TFWO, the population is divided into groups and the best member is set in

the center of the whirlpool. The applied method is characterized by centrifugal force which affects on randomly selected dimensions of the decision variables after evaluating the fitness of the objects. In addition to affecting objects, whirlpools also interact with each other.

3.2. Objective function

The parameters of the PID controller undoubtedly influence the dynamic behaviour of the control system by shaping the control signal. In order to determine the desired dynamics of the response of the controlled object, there is a need to evaluate it in qualitative and quantitative terms. Such an evaluation is typically carried out using control quality indexes, which can take different forms depending on the objective pursued. Typical quality indexes that can be obtained directly from the behaviour of the controlled variable are: settling time, oscillation damping, peak response or rise time. Another group of control quality indexes belong to the family of so called integral quality indexes. These indexes are directly related to minimization the differences between the two selected time functions in the control system. Typically these functions are defined as a reference value and a controlled value for the tracking task, and the difference between them is the control error. The task of the overall quality indicators is to clearly define the distance (standard) of the functions to be taken into account from the timeline, especially when this function repeatedly intersects the timeline [11]. Four integral indexes were considered in further work:

1. The integral of absolute error (IAE):

$$IAE = \int_{t_0}^{t_e} |e(t)| dt. \quad (6)$$

2. The integral of square error (ISE):

$$ISE = \int_{t_0}^{t_e} e^2(t) dt. \quad (7)$$

3. The integral of time multiply absolute error (ITAE):

$$ITAE = \int_{t_0}^{t_e} |e(t)| t dt. \quad (8)$$

4. The integral of time multiply absolute error (ITSE)

$$ITSE = \int_{t_0}^{t_e} t e^2(t) dt; \quad (9)$$

where: t_0 is start time and t_r is end time of the simulation.

3.3. Scheme of PID controller parameters process

The scheme of the PID controller parameters selection process is presented in Fig. 9. Using selected optimization methods, the best parameters of the PID controller were searched for. This process was based on predefined objective functions (6)-(9). In order to compare the applied optimization methods accurately and reliably, 10 simulations of the optimization of PID controller parameters for each algorithm were performed. This procedure was aimed at averaging the results resulting from the stochastic nature of the investigated algorithms. On the basis of the simulations carried out, the mean values of the objective function and the standard deviation values were determined. Table 4 presents the basic values of the hyperparameters of the tested optimization algorithms which suggested by authors. The optimization process was carried out using available functions

in Matlab/Simulink environment and those written by the authors on their own. The value of the objective functions was derived from the response of the control system using a mathematical model of the sliding bearing, which was developed in the Simulink environment and presented in section Bearing model designing in Matlab SIMULINK environment.

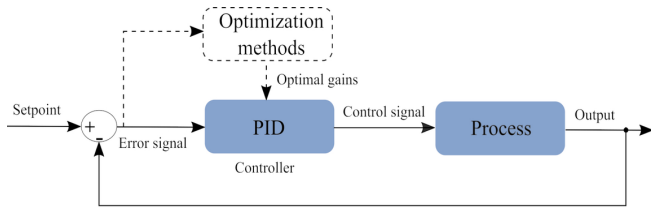


Fig. 9. Structure of the optimization methods to optimize the controller parameters

Table 4. Hyperparameters of optimization algorithms used

| Parameter | Symbol | Value |
|-------------------------------|------------------------------------|-------|
| Population size | N (All algorithms) | 30 |
| Dimension | d (All algorithms) | 3 |
| Iteration number | Max _{it} (All algorithms) | 20 |
| Inertia weight | <i>in</i> (PSO) | 1 |
| Inertia weight damping ratio | <i>w_d</i> (PSO) | 0.99 |
| Personal learning coefficient | <i>c₁</i> (PSO) | 1.5 |
| Global learning coefficient | <i>c₂</i> (PSO) | 2 |
| Velocity | <i>v</i> (PSO) | 2 |
| Inertia maximum weight | <i>w_{max}</i> (TACPSO) | 0.9 |
| Inertia minimum weight | <i>w_{min}</i> (TACPSO) | 0.4 |

4. Results

A series of calculations of PID controller parameters optimization designed to control the radial sliding bearing was carried out to determine the most effective optimization algorithm for this task. The calculations were made for four different integral objective functions commonly used in the search of optimal PID controller parameters. To make an accurate comparison of the effectiveness or efficiency of optimization algorithms, it is necessary to compare them in a way that allows a detailed analysis of the work. Therefore, the charts include function evaluations as function arguments. The adopted methodology allows to eliminate any complexities related to the specificity of a given algorithm behaviour and reliable evaluation in relation to other algorithms, which could occur if the iteration function of the algorithm is included as an argument. Table 5 summarizes the results of optimization for the target function defined by IAE. The best (minimum) value of the target function, mean and standard deviation for all the optimization attempts are presented. The satisfactory results were obtained in all the algorithms used, but the average value of the target function was much higher in the genetic algorithm (GA) and in chimp algorithm (ChOA). Noteworthy is the GWOCS algorithm, by which the smallest value of standard deviation was obtained. The relative difference between the best solution and the second best solution (PSO) was more than 360%. Fig. 10 presents the course of improving the value of the target function for optimal values given in Table 5. The number of function calls necessary to achieve the minimum objective function values did not exceed 200. In the case of a genetic algorithm, a minimum of the objective function was achieved very quickly (about 50 iterations less than the second results), but this did not coincide with the rest of the trials for this algorithm, which

consequently resulted in a higher standard deviation value (penultimate result). Tables 6-8 show the results of optimization for the target function defined by ISE, ITAE and ITSE. For all algorithms and objective functions used, the satisfactory results were obtained. Among the swarm algorithms, the best results were obtained for the particle swarm algorithm, while among the hybrid algorithms, the GWOCS algorithm turned out to be the best choice, in case of which also the best results among all the applied algorithms were obtained. Target function improvement courses (Fig. 10-13) showed much faster target function improvement by stochastic algorithms, but the repeatability of these results was much lower than for hybrid algorithm. The hybrid algorithm needs an average of 30% more iterations but achieves an average standard deviation error concerning the second-best value less than 7.45E-06.

Table 5. Optimization results for objective function defined by IAE

| Algorithm | Best value | Mean value | Standard deviation |
|-----------|--------------|--------------|--------------------|
| GA | 8.151634E-02 | 8.668518E-02 | 4.957340E-03 |
| PSO | 8.145061E-02 | 8.146491E-02 | 5.850000E-06 |
| WOA | 8.144845E-02 | 8.146373E-02 | 1.288000E-05 |
| GWOCS | 8.145603E-02 | 8.145757E-02 | 1.270000E-06 |
| TCAPSO | 8.144773E-02 | 8.145402E-02 | 1.109000E-05 |
| ChOA | 8.144778E-02 | 8.502151E-02 | 5.724320E-03 |
| TFWO | 8.144772E-02 | 8.145094E-02 | 8.030000E-06 |

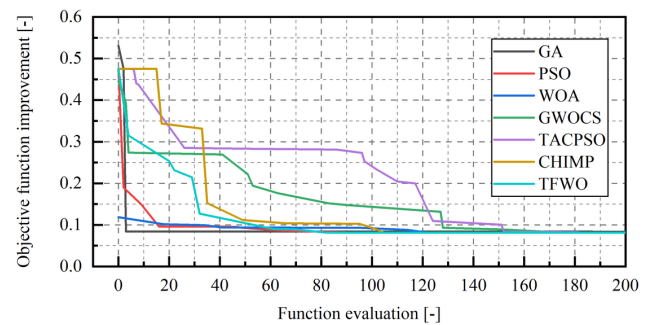


Fig. 10. Course of improvement of objective function value (IAE)

Table 6. Optimization results for objective function defined by ISE

| Algorithm | Best value | Mean value | Standard deviation |
|-----------|--------------|--------------|--------------------|
| GA | 2.650354E-02 | 3.311707E-02 | 1.104383E-02 |
| PSO | 2.650084E-02 | 2.651836E-02 | 2.809000E-05 |
| WOA | 2.649465E-02 | 2.784310E-02 | 4.247450E-03 |
| GWOCS | 2.649667E-02 | 2.650112E-02 | 2.850000E-06 |
| TCAPSO | 2.649532E-02 | 2.649853E-02 | 2.280000E-06 |
| ChOA | 2.649737E-02 | 2.820079E-02 | 3.754650E-03 |
| TFWO | 2.649356E-02 | 2.649700E-02 | 2.260000E-06 |

In order to confirm the correctness of the optimization process, the simulation of the radial sliding bearing control system with the obtained PID controlled parameters was repeated. The plots of the control signal values for each algorithm and for each defined objective function were plotted. The results are presented in Fig. 14. The resulting plots are similar to each other (for each objective function) and, regardless of the algorithm or target function used, reach the assumed

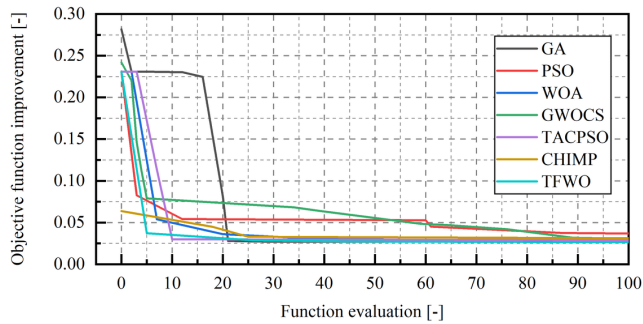


Fig. 11. Course of improving objective function (ISE)

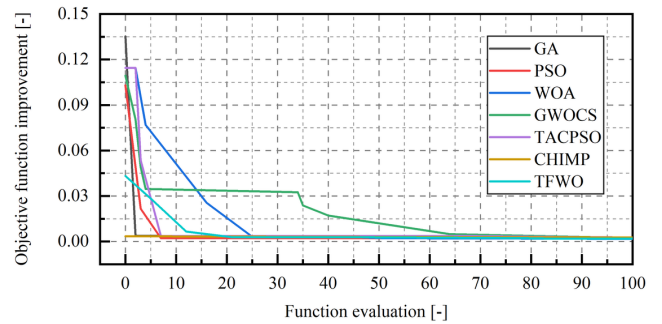


Fig. 13. Course of improvement of objective function (ITSE)

Table 7. Optimization results for the objective function defined by ITAE

| Algorithm | Best value | Mean value | Standard deviation |
|-----------|--------------|--------------|--------------------|
| GA | 7.299040E-03 | 1.471883E-02 | 1.398233E-02 |
| PSO | 7.295020E-03 | 7.296960E-03 | 9.700000E-07 |
| WOA | 7.293010E-03 | 7.324610E-03 | 3.672000E-05 |
| GWOCS | 7.292630E-03 | 7.294000E-03 | 1.110000E-06 |
| TCAPSO | 7.292590E-03 | 7.294940E-03 | 1.570000E-06 |
| ChOA | 7.292200E-03 | 7.606770E-03 | 9.864100E-04 |
| TFWO | 7.291090E-03 | 7.294380E-03 | 1.660000E-06 |

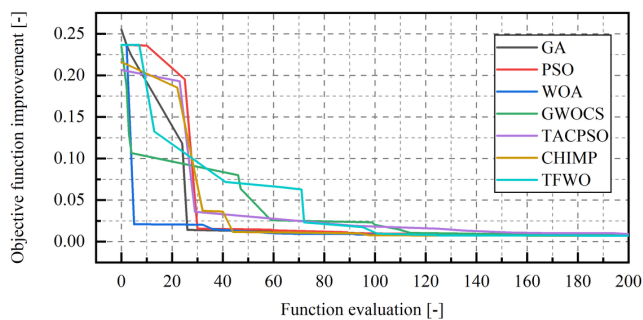


Fig. 12. Course of improving objective function (ITAE)

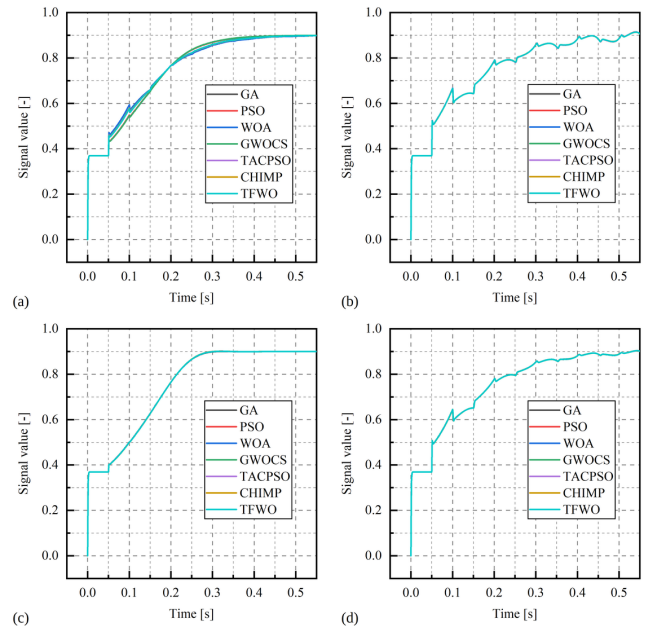


Fig. 14. Value of the radial sliding bearing control signal: a) IAE, b) ISE, c) ITAE, d) ITSE

Table 8. Optimization results for objective function defined by ITSE

| Algorithm | Best value | Mean value | Standard deviation |
|-----------|--------------|--------------|--------------------|
| GA | 1.799870E-03 | 2.665530E-03 | 1.944100E-03 |
| PSO | 1.799450E-03 | 1.800210E-03 | 4.800000E-07 |
| WOA | 1.799180E-03 | 1.844380E-03 | 1.406300E-04 |
| GWOCS | 1.798830E-03 | 1.799620E-03 | 3.900000E-07 |
| TCAPSO | 1.799140E-03 | 1.844160E-03 | 1.407100E-04 |
| ChOA | 1.799010E-03 | 2.210660E-03 | 3.568600E-04 |
| TFWO | 1.798670E-03 | 1.843700E-03 | 1.408700E-04 |

value. In addition, they are characterized by a lack of overshoot and a gentle build-up. The adjustment time for all runs is almost identical. It should be mentioned that the system assumes a limitation of the controller's operation, which lead to similar results of the characteristics of the control signal.

5. Conclusion

The method of selection of the parameters of PID controller designed to control the radial sliding bearing is considered this paper, as well as the models of the sliding bearing and the control system were analysed. Attention must be paid to the values of damping and stiffness coefficients that are derived from experimental research, which increases the value of the bearing model and enables a more accurate representation of the actual system. A number of optimization methods were tested, of which one was recommended for further use in this type of solutions. The GWOCS hybrid algorithm turned out to be the most effective, since it maintained a constant high performance regardless of the applied target function. The results show that among swarm algorithms, the particle swarm algorithm (PSO) is the best. In turn, in all the analyses carried out, the genetic algorithm was the worst.

An active foil bearing can help prevent damage to the entire rotating system. Random events occur in rotating machines, for example, a blade breakage, and thus an increase in the unbalance of the system. Another example would be misalignment or damage, for instance, support elements. These events are usually associated with an increase in the amplitude of vibrations. The parameters of the PID controller, which were selected in the optimization process shown, determine how quickly the bearing will react, what will be the overload and, as

a result, how the active foil bearing will help to avoid damage to the entire rotating system.

The described results will be proposed for implementation and validation in active foil bearing system constructed by authors.

Acknowledgements

This paper was created within the framework of the ACTIVER-ING project entitled “Aktywne łożyska foliowe ze zmiennymi właściwościami dynamicznymi” (Eng. Active foil bearings with variable dynamic properties), agreement no. LIDER/51/0200/L9/17/NCBR/2018, implemented as part of the research and development program called “LIDER” (Eng. LEADER).

Calculations were carried out at the Academic Computer Center in Gdansk.

References

1. Abdulameer A, Sulaiman M, Aras M S M, Saleem D. Tuning methods of PID controller for DC motor speed control. *Indonesian Journal of Electrical Engineering and Computer Science* 2016; 3(2): 343–349, <https://doi.org/10.11591/ijeecs.v3.i2.pp343-349>.
2. Ahmad I, Shahzad M, Palensky P. Optimal PID control of Magnetic Levitation System using Genetic Algorithm. 2014 IEEE International Energy Conference (ENERGYCON), 2014: 1429–1433, <https://doi.org/10.1109/ENERGYCON.2014.6850610>.
3. Åström K J, Häggglund T. PID controllers: theory, design, and tuning. 2nd edition. Research Triangle Park, Instrument society of America: 1995: 354.
4. Åström K J, Panagopoulos H, Häggglund T. Design of PI controllers based on non-convex optimization. *Automatica* 1998; 34(5): 585–601, [https://doi.org/10.1016/S0005-1098\(98\)00011-9](https://doi.org/10.1016/S0005-1098(98)00011-9).
5. Bahavarnia M, Tavazoei M S. A new view to Ziegler–Nichols step response tuning method: Analytic non-fragility justification. *Journal of Process Control* 2013; 23(1): 23–33, <https://doi.org/10.1016/j.jprocont.2012.10.012>.
6. Barbosa R S, Machado J A T, Ferreira I M. Tuning of PID controllers based on bode’s ideal transfer function. *Nonlinear Dynamics* 2004; 38(1–4): 305–321, <https://doi.org/10.1007/s11071-004-3763-7>.
7. Blaut J, Breńkacz Ł. Application of the Teager–Kaiser energy operator in diagnostics of a hydrodynamic bearing. *Eksploatacja i Niezawodność - Maintenance and Reliability* 2020; 22(4): 757–765, <https://doi.org/10.17531/ein.2020.4.20>.
8. Breńkacz Ł, Szewczuk-Krypa N, Witanowski Ł, Drosińska-Komor M. The basic control model of an active foil bearing. *The Proceedings of the International Conference on Motion and Vibration Control* 2020; 2020.15: 10033, <https://doi.org/10.1299/jsmeintmovic.2020.15.10033>.
9. Breńkacz Ł, Witanowski Ł, Drosińska-Komor M, Szewczuk-Krypa N. Research and applications of active bearings: A state-of-the-art review. *Mechanical Systems and Signal Processing* 2021; 151: 107423, <https://doi.org/10.1016/j.ymssp.2020.107423>.
10. Breńkacz Ł, Witanowski Ł, Drosińska-Komor M, Szewczuk-Krypa N. Research and applications of active bearings: A state-of-the-art review. *Mechanical Systems and Signal Processing* 2021; 151: 107423, <https://doi.org/10.1016/j.ymssp.2020.107423>.
11. Byrski W. *Observacja i sterowanie w systemach dynamicznych*. 1st edition. Uczelniane Wydaw. Naukowo-Dydaktyczne AGH: 2007: 314.
12. Castilla-Gutiérrez J, Fortes J C, Davila J M. Control and prediction protocol for bearing failure through spectral power density. *Eksploatacja i Niezawodność - Maintenance and Reliability* 2020; 22(4): 651–657, <https://doi.org/10.17531/ein.2020.4.8>.
13. Chen H, Chang S. Genetic Algorithms Based Optimization Design of a PID Controller for an Active Magnetic Bearing. *IJCSNS International Journal of Computer Science and Network Security* 2006; 6(12): 95–99.
14. Chen K-Y Y, Tung P-C C, Tsai M-T T, Fan Y-H H. A self-tuning fuzzy PID-type controller design for unbalance compensation in an active magnetic bearing. *Expert Systems with Applications* 2009; 36(4): 8560–8570, <https://doi.org/10.1016/j.eswa.2008.10.055>.
15. Chen X, Przystupa K, Ye Z et al. Forecasting short-term electric load using extreme learning machine with improved tree seed algorithm based on Lévy flight. *Eksploatacja i Niezawodność - Maintenance and Reliability* 2022; 24(1): 153–162, <https://doi.org/10.17531/ein.2022.1.17>.
16. Chien I, Hrones J, Reswick J. On the automatic control of generalized passive systems. *Trans. ASME* 1952: 175–185.
17. Couzin I D, Laidre M E. Fission-fusion populations. *Current Biology* 2009; 19(15): 633–635, <https://doi.org/10.1016/j.cub.2009.05.034>.
18. Eberhart R, Kennedy J. New optimizer using particle swarm theory. *Proceedings of the International Symposium on Micro Machine and Human Science* 1995: 39–43, <https://doi.org/10.1109/mhs.1995.494215>.
19. Fan S-K S, Chang J-M. Dynamic multi-swarm particle swarm optimizer using parallel PC cluster systems for global optimization of large-scale multimodal functions. *Engineering Optimization* 2010; 42(5): 431–451, <https://doi.org/10.1080/03052150903247736>.
20. Fan S-K S, Jen C-H. An Enhanced Partial Search to Particle Swarm Optimization for Unconstrained Optimization. *Mathematics* 2019; 7(4): 357, <https://doi.org/10.3390/math7040357>.
21. Fan S K S, Liang Y C, Zahara E. A genetic algorithm and a particle swarm optimizer hybridized with Nelder-Mead simplex search. *Computers and Industrial Engineering* 2006; 50(4): 401–425, <https://doi.org/10.1016/j.cie.2005.01.022>.
22. Fan S K S, Zahara E. A hybrid simplex search and particle swarm optimization for unconstrained optimization. *European Journal of Operational Research* 2007; 181(2): 527–548, <https://doi.org/10.1016/j.ejor.2006.06.034>.
23. Ferfecki P, Zapoměl J. Reducing excessive vibration of rigid rotors mounted with hydrodynamic bearings by controlled excitation of the rotor supports. 2012.
24. Fung H W, Wang Q G, Lee T H. PI tuning in terms of gain and phase margins. *Automatica* 1998; 34(9): 1145–1149, [https://doi.org/10.1016/S0005-1098\(98\)80001-0](https://doi.org/10.1016/S0005-1098(98)80001-0).
25. Ghasemi M, Davoudkhani I F, Akbari E et al. A novel and effective optimization algorithm for global optimization and its engineering applications: Turbulent Flow of Water-based Optimization (TFWO). *Engineering Applications of Artificial Intelligence* 2020; 92(February): 103666, <https://doi.org/10.1016/j.engappai.2020.103666>.
26. Goldberg D E. *Genetic Algorithms in Search, Optimization and Machine Learning*. 1st edition. Addison-Wesley Longman Publishing Co., Inc.: 1989.
27. Hybrid Grey Wolf and Cuckoo Search Optimization Algorithm. [<https://mathworks.com/matlabcentral/fileexchange/69392-hybrid-grey-wolf-and-cuckoo-search-optimization-algorithm>].
28. Heppner F H, Grenander U. A Stochastic Non-Linear Model for Bird Flocking. *The Ubiquity of Chaos* 1990; (January 1990): 233–238.
29. Hernández-Alvarado R, García-Valdovinos L G, Salgado-Jiménez T et al. Neural network-based self-tuning PID control for underwater vehicles. *Sensors (Switzerland)* 2016; 16(9): 1–18, <https://doi.org/10.3390/s16091429>.

30. Jaiswal S, Suresh Kumar C, Seepana M M, Babu G U B. Design of Fractional Order PID Controller Using Genetic Algorithm Optimization Technique for Nonlinear System. *Chemical Product and Process Modeling* 2020; 1–11, <https://doi.org/10.1515/cppm-2019-0072>.
31. Khishe M, Mosavi M R. Chimp optimization algorithm. *Expert Systems with Applications* 2020; 149: 113338, <https://doi.org/10.1016/j.eswa.2020.113338>.
32. Kicinski J. *Rotor Dynamics*. 1st edition. IFFM Publisher: 2006.
33. Korsane D T, Yadav V, Raut K H. PID Tuning Rules for First Order plus Time Delay System. *International Journal Of Innovative Research In Electrical, Electronics, Instrumentation And Control Engineering* 2014; 2(1): 582–586.
34. Lampart P, Yershov S, Rusanov A. Increasing flow efficiency of high-pressure and low-pressure steam turbine stages from numerical optimization of 3D blading. *Engineering Optimization* 2005; 37(2): 145–166, <https://doi.org/10.1080/03052150512331315497>.
35. Maior C B S, das Chagas Moura M, Lins I D. Particle swarm-optimized support vector machines and pre-processing techniques for remaining useful life estimation of bearings. *Eksplatacja i Niezawodnosc - Maintenance and Reliability* 2019; 21(4): 610–619, <https://doi.org/10.17531/ein.2019.4.10>.
36. Manoj K, Ashish P. PID Controller Tuning using Ziegler-Nichols Method for Speed Control of DC Motor. 2014; 03(13): 2924–2929.
37. Mendes J, Osório L, Araújo R. Self-tuning PID controllers in pursuit of plug and play capacity. *Control Engineering Practice* 2017; 69(June): 73–84, <https://doi.org/10.1016/j.conengprac.2017.09.006>.
38. Michalewicz Z. *Genetic algorithms + data structures = evolutionary programmes*. Warszawa, WNT: 1996.
39. Mirjalili S, Lewis A. The Whale Optimization Algorithm. *Advances in Engineering Software* 2016; 95: 51–67, <https://doi.org/10.1016/j.advengsoft.2016.01.008>.
40. Mirjalili S, Lewis A, Sadiq A S. Autonomous Particles Groups for Particle Swarm Optimization. *Arabian Journal for Science and Engineering* 2014; 39(6): 4683–4697, <https://doi.org/10.1007/s13369-014-1156-x>.
41. Morosi S, Santos I F. Experimental Investigations of Active Air Bearings. Volume 7: Structures and Dynamics, Parts A and B, ASME: 2012; (April): 1–10, <https://doi.org/10.1115/GT2012-68766>.
42. Nalepa K, Pietkiewicz P, Żywica G. Development of the foil bearing technology. *Technical Sciences* 2009; 12(1): 229–240, <https://doi.org/10.2478/v10022.009-0019-2>.
43. Olszewski A, Żochowski T, Gołębiowski G. Analysis of the load-carrying capacity of a hydrodynamic water-lubricated bearing in a hydroelectric power plant. *Tribologia* 2018; 278(2): 103–110, <https://doi.org/10.5604/01.3001.0012.6982>.
44. Peng J-P, Carpino M. Finite Element Approach to the Prediction of Foil Bearing Rotor Dynamic Coefficients. *Journal of Tribology* 1997; 119(1): 85–90, <https://doi.org/10.1115/1.2832484>.
45. Pessen D W. A New Look at PID-Controller Tuning. *Journal of Dynamic Systems, Measurement, and Control* 1994; 116(September 1994): 553–557, <https://doi.org/10.1515/9783110862799-032>.
46. Priyambodo T K, Putra A E, Dharmawan A. Optimizing Control based on Ant Colony Logic for Quadrotor Stabilization. 2015. doi:10.1109/ICARES.2015.7429820, <https://doi.org/10.1109/ICARES.2015.7429820>.
47. Psonis T K, Nikolakopoulos P G, Mitronikas E. Design of a PID Controller for a Linearized Magnetic Bearing. *International Journal of Rotating Machinery* 2015.
48. Puchalski B, Duzinkiewicz K, Rutkowski T. Multi-region fuzzy logic controller with local PID controllers for U-tube steam generator in nuclear power plant. *Archives of Control Sciences* 2015; 25(4): 429–444, <https://doi.org/10.1515/acsc-2015-0028>.
49. Puchalski B, Rutkowski T A, Duzinkiewicz K. Fuzzy Multi-Regional Fractional PID controller for Pressurized Water nuclear Reactor. *ISA Transactions* 2020; 103: 86–102, <https://doi.org/10.1016/j.isatra.2020.04.003>.
50. Puchalski B, Rutkowski T, Tarnawski J, Duzinkiewicz K. Comparison of tuning procedures based on evolutionary algorithm for multi-region fuzzy-logi PID controller for non-linear plant. 2015 20th International Conference on Methods and Models in Automation and Robotics, MMAR 2015 2015: 897–902, <https://doi.org/10.1109/MMAR.2015.7283996>.
51. Regad M, Helaimi M, Taleb R et al. Fractional Order PID Control of Hybrid Power System with Renewable Generation Using Genetic Algorithm. *Proceedings of 2019 the 7th International Conference on Smart Energy Grid Engineering, SEGE 2019* 2019: 139–144, <https://doi.org/10.1109/SEGE.2019.8859970>.
52. Singh S S K, Abdullah S, Mohamed N A N. Reliability analysis and prediction for time to failure distribution of an automobile crankshaft. *Eksplatacja i Niezawodnosc - Maintenance and Reliability* 2015; 17(3): 408–415, <https://doi.org/10.17531/ein.2015.3.11>.
53. Siva Srinivas R, Tiwari R, Kannababu C. Application of active magnetic bearings in flexible rotordynamic systems – A state-of-the-art review. *Mechanical Systems and Signal Processing* 2018; 106: 537–572, <https://doi.org/10.1016/j.ymssp.2018.01.010>.
54. Smolinski M, Perkowski T, Mystkowski A et al. AMB flywheel integration with photovoltaic system for household purpose – modelling and analysis. *Eksplatacja i Niezawodnosc - Maintenance and Reliability* 2016; 19(1): 86–94, <https://doi.org/10.17531/ein.2017.1.12>.
55. Tandon B. Genetic Algorithm Based Parameter Tuning of Pid Controller for Composition Control System. *International Journal of Engineering Science and Technology* 2011; 3(8): 6705–6711.
56. Yang X-S. *Recent Advances in Swarm Intelligence and Evolutionary Computation*. Studies in. Springer: 2015. doi:10.1007/978-3-319-13826-8, <https://doi.org/10.1007/978-3-319-13826-8>.
57. Zdziebko P, Martowicz A. Study on the temperature and strain fields in gas foil bearings – measurement method and numerical simulations. *Eksplatacja i Niezawodnosc - Maintenance and Reliability* 2021; 23(3): 540–547, <https://doi.org/10.17531/ein.2021.3.15>.
58. Żywica G, Kaczmarczyk T Z. Experimental evaluation of the dynamic properties of an energy microturbine with defects in the rotating system. *Eksplatacja i Niezawodnosc - Maintenance and Reliability* 2019; 21(4): 670–678, <https://doi.org/10.17531/ein.2019.4.17>.